

Road Vehicle Recognition Using Magnetic Sensing Feature Extraction and Classification

Xiao Chen, Xiaoying Kong, Min Xu

Abstract—This paper presents a road vehicle detection approach for the intelligent transportation system. This approach mainly uses low-cost magnetic sensor and associated data collection system to collect magnetic signals. This system can measure the magnetic field changing, and it also can detect and count vehicles. We extend Mel Frequency Cepstral Coefficients to analyze vehicle magnetic signals. Vehicle type features are extracted using representation of cepstrum, frame energy, and gap cepstrum of magnetic signals. We design a 2-dimensional map algorithm using Vector Quantization to classify vehicle magnetic features to four typical types of vehicles in Australian suburbs: sedan, VAN, truck, and bus. Experiments results show that our approach achieves a high level of accuracy for vehicle detection and classification.

Keywords—Vehicle classification, signal processing, road traffic model, magnetic sensing.

I. INTRODUCTION

INTELLENT transportation systems (ITS) deploy sensors to collect and analyze road vehicle information for road vehicle monitoring, data analysis, managing, control of road traffic, and data analysis for future development of transportation infrastructures. The road traffic information includes: passing vehicle location, vehicle type, vehicle speed and direction, vehicle weight, and vehicle volume in certain zones [1], [2].

The first traffic monitor sensor was developed and installed for road use in 1928. This device used a microphone to detect vehicle sound [1]. Since then, road vehicle sensing technologies have been explored in vibration, inductive-loop detecting, magnetic field, acoustic sensing, optical and infrared sensing, satellite signal processing, camera image and video processing, and inertial sensing [1], [2]. Sensing technologies can be utilized in single sensor, or sensor network.

In this paper, we present a road vehicle identification and classification approach using roadside-installed single magnetic sensor. The magnetic sensor measures the magnetic field changes when vehicle passing. The sensor measurement signals are analyzed to extract vehicle features, and these features are classified into vehicle types. Major passing vehicles on road traffic are therefore detected for four types of vehicles: Sedan, VAN, Truck, and Bus.

From deployment perspective, this magnetic sensing and detection approach does not require road traffic interruption

for installation and maintenance and can be applied in day and night conditions. On detection algorithm side, we extend the feature extraction and classification process from video signal approach. The experiments have validated this approach. This approach can be applied to intelligent transportation system to provide dynamic information of road vehicle types, and traffic flow conditions.

This paper is organized as follows. Section II reviews related work in vehicle detecting and classification. Section III presents the experimental design for magnetic sensing in this research. Section IV presents an algorithm for vehicle identification and vehicle type classification. The results of the road vehicle identification and classification are demonstrated and evaluated in Section V. Conclusions are drawn finally.

II. RELATED WORK

In the previous work, there are different types of sensors, such as radar, infrared, camera, magnetic sensor and so on, vehicle measurement could be detected by various sensors and vehicle's parameters in length, height and width dimensions are extracted to for images and used these features to classify vehicle types [3]. These sensors detect different signal wave, images and frequency. While magnetic sensors measure the magnetic field. Magnetic sensing technologies include: squid, fiber-optic, optical pumped, nuclear procession, search-coil, anisotropic magneto-resistive, flux-gate, etc. [4]. The impact of vehicle passing or stopping to the earth magnetic field change is within the range of 1 μ G to 10 G [4]. In the below, these sensors will be introduced, and we use the AMR sensor as our tool to detect and collect the vehicle data in this report.

In radar sensor, the major radar detection can be summarized into two types: microwave (MW) radar and millimeter wave (mmW) sensor. Firstly, in the mmW sensor, the feature is electromagnetic (EM) backscattering fields from the target, and the echo signals will be received by the radar system. The vehicle can be well performed by the incident beams. Due to the metal structures being relative with EM scattering, the side-front part is very important factor. The analysis of these two vehicles perform the information of effectiveness of radar detection in vehicle. In [5], operation frequency is set at 24.125 GHz. The distance between the antennas and vehicles is 4.7 meters. The positions relative to the vehicles' positions are varied to simulate the scenario of a moving vehicle. And we fix the vertical location of antenna at 2.55 m. In the experiment, the narrow beam demonstrates a small part of vehicles and causes false detections. The AMASM method is applied to smooth out the patterns of backscattering fields, which could effectively reduce the

Xiao Chen, Xiaoying Kong, and Min Xu are with the faculty of Engineering and Information Technology, University of Technology Sydney, Australia (e-mail: Xiao.Chen-8@student.uts.edu.au, xiaoying.kong@uts.edu.au, min.xu@uts.edu.au).

possibility of false detection and recognition. While in the microwave (MW) radars, it needs to satisfy certain requirements, firstly, radiation pattern needs wide road coverage transverse to traffic flow and narrow coverage along the traffic flow. In addition, high distance resolution and sampling frequency make sure that signals satisfy this requirement. Lastly, we provide a wide dynamic range according to the return amplitudes.

In infrared (IR) sensor, the infrared system also could detect vehicles and it includes paired transmitter (Tx) and receiver (Rx) array that is mounted horizontally and vertically [6]. When a vehicle went across the Tx and Rx towers, raw data are transformed into per blockage of the infrared sensors for that certain timer, all these similar pulse cycles collectively produce profile of a vehicle that is useful for vehicle numbering and category [7]. IR LED driver could be transistorized switching circuit which could transmit the train of pulse at individual level in synchronization with Rx controller. The output of the IR sensor could recognize the particular sensor. Then, the vehicle profile generator will receive raw data from the output IR LED, and it create the graphical profile of vehicles. Vehicle classification is based on multiple combinations of the extracted data, when processing and generating the profile of the vehicle. As in vehicle classification, the classification rule can be defined as valve selection and the output is three kinds of vehicles, including bus, truck and car.

In camera sensor, cameras sensors are multiple cameras. In [8], firstly, each camera can extract one image patch per vehicle, which is a vehicle patch. Then, color information into consideration, we extract features based on Harris corner detection with Opponent SIFT descriptors, a Spatiotemporal Successive Dynamic Programming (S2DP) algorithm for multiple cameras is put forward to identify vehicles. For performance evaluation and comparison, there are four approaches in implement and test, including: firstly, the proposed S2DP algorithm, then the proposed S2DP algorithm without the consideration of the penalty A for non-successive assignment, followed by the baseline Hungarian algorithm, and lastly the state-of-the-art approach proposed by Cabrera et al. while the average accuracy of performance of S2DP on vehicle are below 75%, and this paper only detects the vehicle rather than classification the different types of vehicles.

Comparing with other types of magnetic field sensing technologies in range and cost, Anisotropic Magneto-resistive (AMR) sensors are able to work in this range of magnetic field changes for practical application. As we discussed, there are environment limitations about above sensors, such raining or foggy weather. The performance will be dramatically influenced, and the accuracy will decrease. The magnetic field change measurements of AMR sensors used in road experiments are analyzed using vehicle detecting and classification approaches. Signal analysis of magnetic field measurement and classifying into signal shape patterns has been an effective approach.

Our approach is presented in the following sections.

III. EXPERIMENT DESIGN USING MAGNETIC SENSOR IN ROAD TRAFFIC

In Australia, vehicles travel on left side of a road. Our experiments were conducted on a road in Sydney suburb. The types of observed vehicle on this road are: Sedan, VAN, Truck and Bus. We used a single 3-axle AMR sensor to measure the earth magnetic field changes when vehicles were passing our experiment area. The road experiment is configured as in Fig. 1.

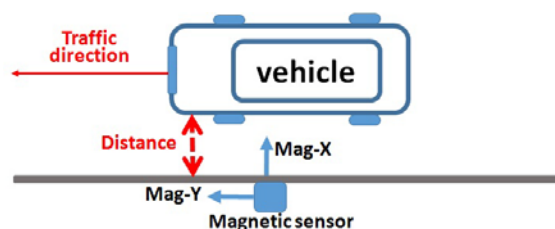


Fig. 1 Road experiment configuration

The AMR sensor is mounted on roadside. The distance between passing vehicles and the road is about 60 cm. Axis-Y of the sensor is pointing to the direction of traffic flow, parallel to the roadside. Axis-X is pointing to the vehicle, vertically to Axis-Y. Axis-Z is pointing up. The AMR sensor outputs three measurements as Mag-X, Mag-Y and Mag-Z. The unit of the sensor measurement is μG in our experiment. The measurements of magnetic field are in time domain. The passing vehicle types, and vehicle passing time period are recorded. The collected measurement data were used offline to analyze the types of vehicles.

The identification and classification of vehicles are presented in the next section.

IV. VEHICLE CLASSIFICATION ALGORITHM

In our research, we analyze Mel Frequency Cepstral Coefficients (MFCC) for audio systems and Vector Quantization (VQ) to analyze magnetic field measurement data for passing vehicles. Audio features of MFCC represent the characteristic of human sound system [11], [12]. Vector Quantization is lossy data compression method for audio signals. VQ can transform several scalar data into one vector data, and quantize whole vector space [13], [14].

In identification and classification of vehicle signals, we extract features first, and classify the features to different types of vehicles. The process is presented below.

A. Feature Extraction Process

In literature, MFCC was used to extract speech signal feature in speech recognition systems [9], [10]. Audio signal features include speech speed, speech fragment length, speech frequency, and amplitude.

The process flow of the magnetic field features extraction is described in Fig. 2.

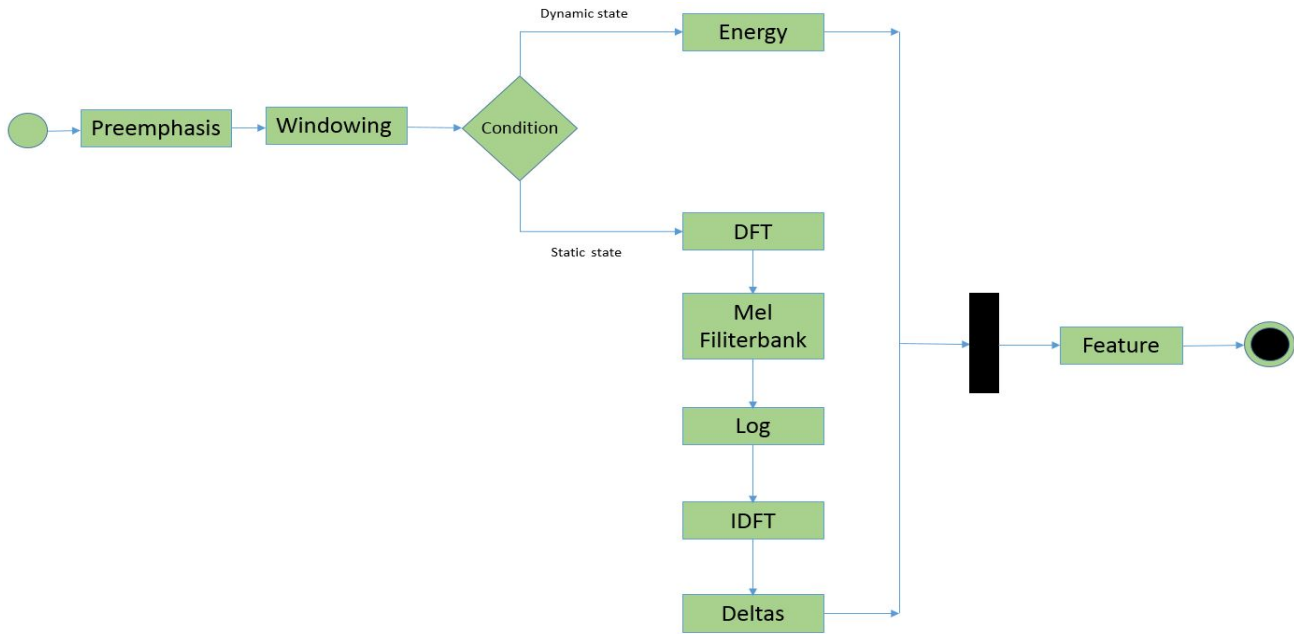


Fig. 2 Magnetic measurement feature extraction

1. Preemphasis

The first step of magnetic signal feature extraction is “preemphasis”. This step improves the energy in high frequencies and balances the energy from lower and higher frequencies. In the time domain, the filter equation is as:

$$y[n] = x[n] - \alpha x[n-1]. \quad (1)$$

where, n is the time, $x[n]$ is the input signal, and $0.9 \leq \alpha \leq 1$.

2. Windowing

In the second step “Windowing”, we extract signal feature from a small window of signal. The windowing process is performed using signal value and window value. If the value of the signal at time n is $s[n]$, the value of the window at time n is $w[n]$, the signal value $y[n]$ of this windowing process is presented as:

$$y[n] = w[n]s[n]. \quad (2)$$

In order to shrink the values of the signal toward zero at the window boundaries and avoid discontinuities, we define two windowing functions: “Rectangular” and “Hamming”.

3. “Rectangular”:

We set the window to 1 when signal time n is between 0 and $L-1$, L is the length of the frame of the signal. In other time period, we set window to 0 [9], [10].

$$w[n] = \begin{cases} 1 & 0 \leq n \leq L-1 \\ 0 & \text{otherwise} \end{cases}. \quad (3)$$

4. “Hamming”:

Hamming window is the goal to extract the spectral features, not from the entire signal, it can extract spectral features from a small window of signal [10].

$$w[n] = \begin{cases} 0.54 - 0.46 \cos \frac{2\pi n}{L} & 0 \leq n \leq L-1 \\ 0 & \text{otherwise} \end{cases}. \quad (4)$$

After the “Windowing” process, the distributed frames will result in two states: dynamic state and static state. The feature extracting process will go through two different flows as in Fig. 2. After “Windowing” processing, there is a condition to process each frame in magnetic feature, and there are two steps including dynamic and static site, due to the reason of each frame in “Windowing”.

The windowing process includes “frame shift” and “frame size”. We hardly to extract entire feature from the magnetic feature, because the spectrum changes very fast. Therefore, in the frame state, there are two conditions: *dynamic state* and *static state* to resolve this issue. The *dynamic* processing is caused by frame shift that is 10 ms, while the *static* state is frame size, which is 25 ms. Therefore, the total feature is the data of dynamic and static.

5. Discrete Fourier Transform (DFT)

For static frame condition, the third step is Discrete Fourier Transform (DFT). We extract magnetic information for windowed signal. We calculate how much energy the signal contains at different frequency bands.

The DFT is defined as:

$$x[k] = \sum_{n=0}^{N-1} x[n] e^{-j2\frac{\pi}{N}kn}. \quad (5)$$

where k and N are the sequence of frame and discrete frequency bands respectively, e , θ are presented in Euler’s formula:

$$e^{j\theta} = \cos \theta + j \sin \theta. \quad (6)$$

6. Mel Filter Bank

The next steps of feature extraction are “Mel Filter Bank” and “Log Processing” to reduce to lower amplitudes. This is computed using:

$$mel(f) = 1127 \ln \left(1 + \frac{f}{700} \right). \quad (7)$$

where f is the frequency of the input signal.

The final steps are “Inverse Discrete Fourier Transform” (IDFT) and “Deltas” and “Energy”: therefore, the magnetic feature includes Cepstrum, Deltas and Energy.

7. Inverse Discrete Fourier Transform (IDFT)

IDFT is computed using the following equations:

$$c[n] = \sum_{k=0}^{N-1} \log \left(\left| \sum_{n=0}^{N-1} x[n] e^{-j \frac{2\pi}{N} kn} \right| \right) e^{j \frac{2\pi}{N} kn}. \quad (8)$$

where c is the cepstrum of magnetic feature.

8. Delta

In Delta stage, we compute the gap cepstrum. Gap cepstrum is defined as the value of average of current cepstrum and the cepstrum of next time. Gap cepstrum d is computed as below.

$$d(t) = \frac{c(t+1) - c(t-1)}{2}. \quad (9)$$

Dynamic state:

For the dynamic state frames after “Windowing”, we start

“Energy” process as in Fig. 2.

9. Energy

Energy is computed using the energy of the frame between two time points, t_1 and t_2 .

$$Energy = \sum_{t=t_1}^{t_2} x^2[t]. \quad (10)$$

10. Feature

For both process flows for dynamic state and static state as in Fig. 3, the final features are integrated.

Magnetic feature is presented using integration of cepstrum c , Energy, and the gap cepstrum d as in (8)-(10).

Vehicle magnetic features are consequently extracted and represented in this process.

B. Vehicle Feature Classification Process

To classify magnetic sensor signals for vehicle types, we transform several scalar magnetic measurement data into one vector. We design this vector containing cepstrum c , Energy, and the gap cepstrum d , which are extracted from the vehicle magnetic feature extraction process.

A vector space is quantized using all magnetic feature vectors. We compress data and store this feature information in magnetic vector space [14].

We design this classification process as shown Fig. 3.

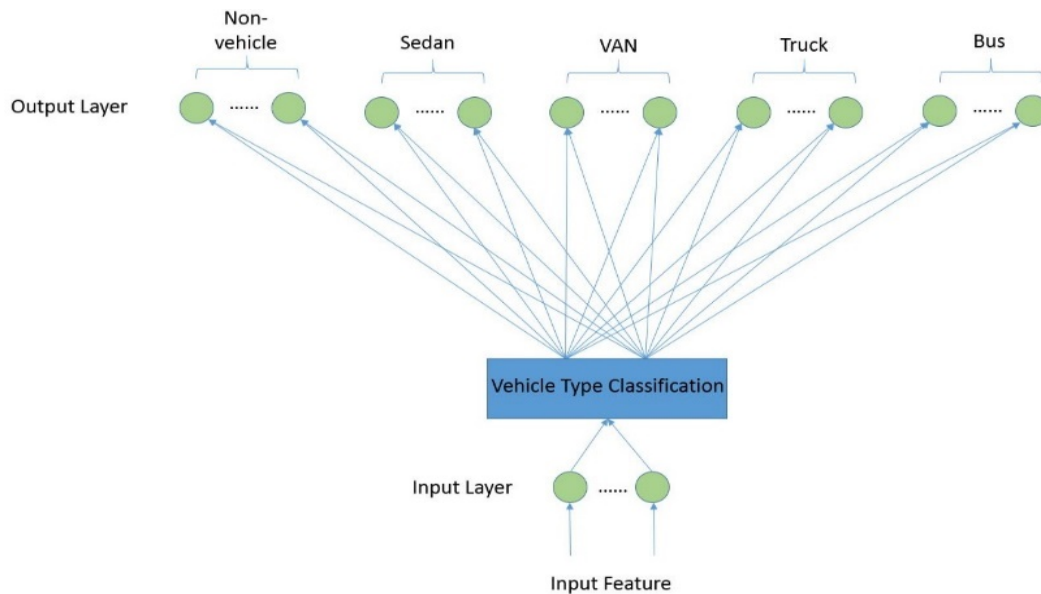


Fig. 3 Vehicle magnetic feature vector quantization classification process

When there is no vehicle in measurement area, magnetic sensor output signals are the earth magnetic field and environment noises. In this process, we define a “Non-vehicle” type when vehicles are absent.

In our experiments, the signal types are: Sedan, VAN, truck, bus and non-vehicle.

We design a 2-dimensional classification map to present the distribution of vehicle types as shown in Fig. 4.

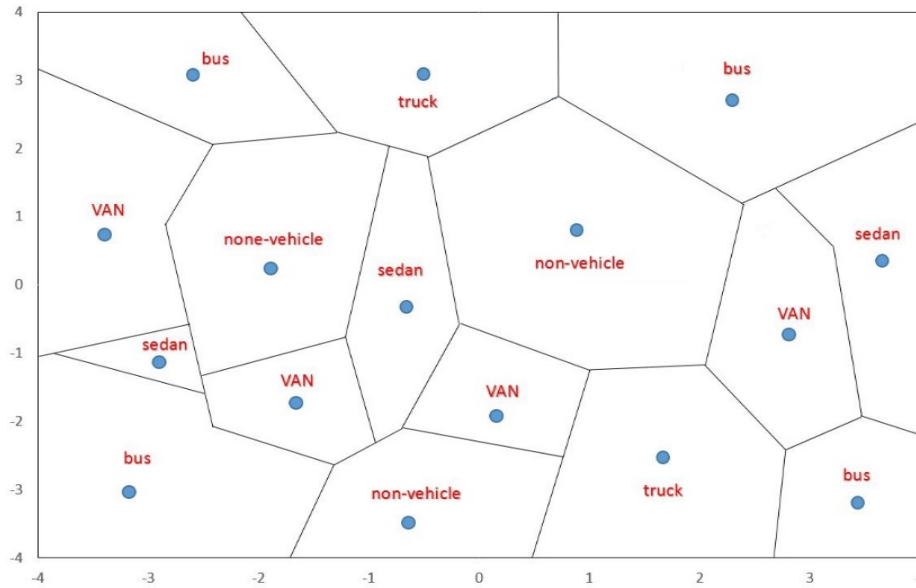


Fig. 4 Distribution of vehicles on 2-dimensional classification algorithm

In this distribution map, we design a pair of numbers as the coordinate. The coordinate is displayed in one region at an approximated position by a blue circle in that region. We uniquely represent each region by this coordinate. For example, we design the coordinate $[-0.5, 0]$ to allocate the position of one passing Sedan in this distribution.

There are 16 regions and 16 blue circles as shown in Fig. 4. In the classification algorithm, we label vector data for feature classification training as $T = \{x_1, x_2, \dots, x_m\}$. We use 2/3 of the entire magnetic feature data as training data. Divide the magnetic feature vector space (classification) to N (5) parts. Let $C = \{c_1, c_2, \dots, c_N\}$ represent a codebook, where c is the codevector. This codebook contains the entire magnetic feature vectors. S_n is the encoding region with codevector c_n . We set entire vector space $P = \{S_1, S_2, \dots, S_N\}$. If X_m is in S_n area, therefore, it can be approximately regarded as c_n : $Q(x_m) = c_n$. We define distortion of magnetic vector that obtains the original vector, instead of changed vector, in order to acquire accurate output data.

The average distortion D_{ave} can be computed using

$$D_{ave} = \frac{1}{Mk} \sum_{m=1}^M |x_m - Q(x_m)|^2. \quad (11)$$

We design optimality criteria using “Nearest Neighbor Condition” and “Nearest Neighbor Condition”.

These criteria are presented as follows:

“Nearest Neighbor Condition”:

$$S_n = \{x: |x - c_n|^2 \leq |x - c_{n'}|^2 \forall n' = 1, 2, \dots, N\}. \quad (12)$$

The vectors standing on boundary can be chosen to certain region S_n .

“Centroid Condition”:

$$c_n = \frac{\sum_{x_m \in S_n} x_m}{\sum_{x_m \in S_n} 1} \quad n = 1, 2, \dots, N. \quad (13)$$

If the transformed vehicle magnetic vector meets the both “Nearest Neighbor Condition” and “Centroid Condition”, then the magnetic vector can be classified into that vehicle type.

V. ANALYSIS OF VEHICLE CLASSIFICATION EXPERIMENT RESULTS

In this section, we perform classification experiments for these vehicle types (Sedan, VAN, Truck, Bus and Non-vehicle) based on signal features obtained from magnetic feature extraction algorithm. In vehicle type classification modelling process, we separate magnetic measurement data into two sets: training data set and testing data set.

We analyzed vehicle type classification using two groups of experiments with six different data configurations.

In Experiment Group 1, we use a dataset of 36 sedans, 8 VANs, 7 trucks, 10 buses and 87 non-vehicle signals.

In Experiment Group 2, we use 73 sedans, 15 VANs, 14 trucks, 15 buses and 174 non-vehicle types of signals.

Table I shows the results of three experiments in Group 1. These results show the observed vehicle type, training data number, testing data number, successful classified vehicle number, and algorithm accuracy in Group 1.

From the results of experiments in Group 1, we find that the algorithm accuracy level is increased when we increase the training data ratio. But if we set the ratio of training dataset and testing data very high, the accuracy level will reach a stable level.

From the results of experiments in Group 1, we find that the algorithm accuracy level is increased when we increase the training data ratio. But if we set the ratio of training dataset and testing data very high, the accuracy level will reach a stable level.

TABLE I
ACCURACY RESULTS OF GROUP 1 EXPERIMENTS

| Group1 | Sedan | | | VAN | | | Truck | | | Bus | | | Non-vehicle | | |
|--------------------------|-------|-----|-----|-----|-----|-----|-------|-----|------|-----|-----|-----|-------------|-----|-----|
| Experiment# | 1 | 2 | 3 | 1 | 2 | 3 | 1 | 2 | 3 | 1 | 2 | 3 | 1 | 2 | 3 |
| Observed | 36 | 36 | 36 | 8 | 8 | 8 | 7 | 7 | 7 | 10 | 10 | 10 | 87 | 87 | 87 |
| Training data | 24 | 27 | 32 | 5 | 6 | 6 | 4 | 5 | 6 | 6 | 7 | 8 | 58 | 66 | 70 |
| Testing data | 12 | 9 | 4 | 3 | 2 | 2 | 3 | 2 | 1 | 4 | 3 | 2 | 29 | 21 | 17 |
| Algorithm classification | 7 | 7 | 5 | 1 | 1 | 1 | 1 | 1 | 1 | 1 | 1 | 1 | 18 | 18 | 14 |
| Algorithm accuracy | 58% | 78% | 75% | 33% | 50% | 50% | 33% | 50% | 100% | 25% | 33% | 50% | 72% | 86% | 82% |

TABLE II
ACCURACY RESULTS OF GROUP 2 EXPERIMENTS

| Group2 | Sedan | | | VAN | | | Truck | | | Bus | | | Non-vehicle | | |
|--------------------------|-------|-----|-----|-----|-----|-----|-------|-----|-----|-----|-----|-----|-------------|-----|-----|
| Experiment# | 1 | 2 | 3 | 1 | 2 | 3 | 1 | 2 | 3 | 1 | 2 | 3 | 1 | 2 | 3 |
| Observed | 73 | 73 | 73 | 15 | 15 | 15 | 14 | 14 | 14 | 15 | 15 | 15 | 174 | 174 | 174 |
| Training data | 48 | 55 | 60 | 10 | 11 | 12 | 9 | 10 | 11 | 10 | 11 | 12 | 116 | 130 | 140 |
| Testing data | 25 | 18 | 13 | 5 | 4 | 3 | 5 | 4 | 3 | 5 | 4 | 3 | 58 | 44 | 34 |
| Algorithm classification | 20 | 15 | 11 | 2 | 2 | 2 | 2 | 2 | 2 | 2 | 2 | 2 | 53 | 40 | 31 |
| Algorithm accuracy | 80% | 83% | 85% | 40% | 50% | 67% | 40% | 50% | 67% | 40% | 50% | 67% | 91% | 91% | 91% |

Table II shows the results using Group 2 experiments.

From the above results of Group 2 experiments, we have 2 findings.

Finding 1. The algorithm accuracy level is increased when we increase the total number of the training data and testing data.

Finding 2. When we increase the ratio of training data and testing data, the accuracy level reaches a stable level.

VI. CONCLUSIONS

In this paper, we present a road vehicle identification and classification approach using magnetic sensor and magnetic signal feature extraction and classification. This approach is designed for analyzing road traffic in intelligent transportation systems.

Using this approach, the installation of magnetic sensor in roadside does not require interruption of road traffic. This reduces the deployment and maintenance cost.

The magnetic signal processing approach extended MFCC to extract the magnetic signal feature and classify the feature to categorize five types of vehicle signals.

Using this approach, we have reached the highest accuracy of vehicle classification in our test data as Sedan 85%, VAN 67%, Truck 67%, Bus 67%, and non-vehicle 91%. In general, our accuracy in test data is: Sedan 80%, VAN 40%, Truck 40%, Bus 40%, and non-vehicle 91%, respectively.

In our future studies, we will aim to increase the classification accuracy by exploring new algorithms.

REFERENCES

- [1] US Department of Transportation (2006) "Federal Highway Administration Research and Technology Coordinating, Developing Highway Transportation Innovations" May 2006.
- [2] Mazarakis Georgios and Avaritsiotis (2007) "Vehicle classification in sensor networks using time-domain signal processing and neural networks", Microprocessors and MICROSYSTEMS, Vol 31. pp 381-392, Feb. 2007.
- [3] Shi, Shengli, Zhong Qin, and Jianmin Xu (2007) "Robust algorithm of vehicle classification", Software Engineering, Artificial Intelligence, Networking, and Parallel/Distributed Computing, 2007. SNPD 2007.

- [4] Eighth ACIS International Conference on. Vol. 3. IEEE, 2007.
- [5] Caruso, Michael J., and Lucky S. Withanawasam. (1999) "Vehicle detection and compass applications using AMR magnetic sensors", Sensors Expo Proceedings. Vol. 477. 1999.
- [6] Chou, Hsi-Tseng & Tuan, Shih-Chung & Ho, Hsien-Kwei. (2016). "Numerical estimation of electromagnetic backscattering from near-zone vehicles for the side-look vehicle-detection radar applications at millimeter waves", IEEE, 129-133. 10.1109.
- [7] Ignacio Llamas-Garro, Konstantin Lukin, Marcos T. de Melo; Jung-Mu Kim, (2016) "Frequency and angular estimation of detected microwave source using aerial vehicles", 2016 IEEE MTT-S Latin America Microwave Conference (LAMC), Puerto Vallarta, Mexico.
- [8] Gajda J. and Stencel M. (2014) "A highly selective vehicle classification utilizing dual-loop inductive detector", Metrology and measurement systems, 2014, 21 (3), pp 473-484.
- [9] Chen, H.-T & Chu, M.-C & Chou, C.-L & Lee, S.-Y & Lin, B.-S. (2015). "Multi-camera vehicle identification in tunnel surveillance system", IEEE. 10.1109.
- [10] Jihyuck Jo, Hoyoung Yoo, and In-Cheol Park (2016) "Energy-Efficient Floating-Point MFCC Extraction Architecture for Speech Recognition Systems", IEEE Trans (VLSI), Vol. 24, No. 2, March 2016.
- [11] Michael Pitz, Ralf Schlüter, and Hermann Ney Sirko Molau (2001) "Computing Mel-Frequency Cepstral Coefficients on the Power Spectrum," in 2001 IEEE International Conference on Acoustics, Speech, and Signal Processing, 2001. Proceedings. (ICASSP '01), USA, 2001, pp. 73-76.
- [12] A. B. Kandali, A. Routray, and T. K. Basu, (2008) "Emotion recognition from assamese speeches using mfcc features and gmm classifier," in TENCON 2008-2008 IEEE Region 10 Conference. IEEE, 2008, pp. 1-5.
- [13] T. F. Quatieri (2002) Discrete-time speech signal processing: principles and practice. Pearson Education India, 2002.
- [14] S. Singh, and E. Rajan (2011) "Vector Quantization approach for speaker recognition using MFCC and inverted MFCC", International Journal of Computer Applications, Vol. 17, No. 1, Mar 2011.
- [15] Gray, Robert. (1984) "Vector quantization." IEEE ASSP Magazine 1.2 (1984): 4-29.